An experimental study of low-pressure premixed pyrrole-oxygen-argon flames with tunable synchrotron photoionization

ARTICLE *in* COMBUSTION AND FLAME · OCTOBER 2007

Impact Factor: 3.08 · DOI: 10.1016/j.combustflame.2007.06.008

6 AUTHORS, INCLUDING:

Zhen-Yu Tian
Chinese Academy of Sciences
66 PUBLICATIONS **889** CITATIONS
SEE PROFILE

Taichang Zhang
Chinese Academy of Sciences
32 PUBLICATIONS **397** CITATIONS
SEE PROFILE

Cui Zhifeng
Anhui Normal University
52 PUBLICATIONS **327** CITATIONS
SEE PROFILE

Available online at www.sciencedirect.com
ScienceDirect
Combustion and Flame 151 (2007) 347–365
Combustion and Flame
www.elsevier.com/locate/combustflame

An experimental study of low-pressure premixed pyrrole/oxygen/argon flames with tunable synchrotron photoionization

Zhenyu Tian [a], Yuyang Li [a], Taichang Zhang [a], Aiguo Zhu [b], Zhifeng Cui [b], Fei Qi [a,*]

[a] *National Synchrotron Radiation Laboratory, University of Science and Technology of China, Hefei, Anhui 230029, People's Republic of China*

[b] *Department of Physics, Anhui Normal University, Wuhu, Anhui 241000, People's Republic of China*

Received 23 January 2007; received in revised form 17 May 2007; accepted 12 June 2007

Available online 31 July 2007

Abstract

Two premixed laminar pyrrole/oxygen/argon flames at 3.33 kPa (25 Torr) with equivalence ratios of 0.55 (C/O/N = 1:5.19:0.25) and 1.84 (C/O/N = 1:1.56:0.25) have been investigated using tunable synchrotron photoionization and molecular-beam mass spectrometry techniques. All observed flame species, including some nitrogen-containing intermediates, have been identified by measurements of photoionization efficiency spectra. Mole fraction profiles of species including reactants, intermediates, and products have been determined by scanning burner position at some selected photon energies near ionization thresholds, and flame temperature has been measured by a Pt/Pt–13% Rh thermocouple. The results indicate that N_2, NO, and NO_2 are the major nitrogenous products, while hydrogen cyanide, isocyanic acid, and 2-propenenitrile are the most important nitrogen-containing intermediates in pyrrole flames. Radicals such as methyl, propargyl, allyl, cyanomethyl, *n*-propyl, isobutyl, cyclopentadienyl, phenyl, cyclohexyl, phenoxy, and 4-methylbenzyl are observed as well. Moreover, ethenol and methylacrylonitrile are also detected. Reaction pathways involving the major species are proposed. The new results will be useful in developing a kinetic model of nitrogenous compound combustion.

Keywords: Pyrrole; Premixed flame; Tunable VUV photoionization; Molecular-beam mass spectrometry; Nitrogen-containing intermediates

1. Introduction

Pyrrole is the most important representative of the five-membered aromatic nitrogenous heterocycles, which can be formed during the decomposition of polypeptides such as casein or gelatin [1,2]. Pyrrole, along with pyridine, is a predominant source of fuel nitrogen in coal and other low-rank fossil fuels and an important component in many oil-based products [3–6]. Its pyrolysis and oxidation reactions are significant for production of precursors of NO_x, which are toxic to human health and conduce to environmental hazards such as acid rain and smog [7]. It

* Corresponding author. Fax: +86 551 5141078.
E-mail address: fqi@ustc.edu.cn (F. Qi).

0010-2180/$ – see front matter
doi:10.1016/j.combustflame.2007.06.008

has been demonstrated previously that the conversion of pyrrole should be taken into account in predicting the formation of NO in the combustion of coals [8]. Thus, studies on pyrrole flames are significant for researchers in understanding the combustion chemistry of nitrogenous fuel and reduce the NO_x emissions.

However, no previous research on combustion of pyrrole has been reported, whereas the photochemistry of pyrrole has been investigated extensively, including photoabsorption [9–12] and photodissociation [13–16] studies, as well as pyrolysis of pyrrole [7,17–19]. Among these, Lifshitz et al. [17] and Mackie et al. [19] found that the major pyrolysis products of pyrrole over the temperature range 1050–1700 K with shock tube technique were HCN, propyne (p-C_3H_4)/allene (a-C_3H_4), crotonitrile ($CH_3CHCHCN$), and allyl cyanide (CH_2CHCH_2CN). They also suggested that these species were formed via a common biradical intermediate. Lifshitz et al. determined Arrhenius parameters of destruction of pyrrole and formation of major products. Mackie et al. carried out a detailed kinetic modeling study and obtained reasonable fits to the observed temperature profiles. Lumbreras et al. studied oxidation of pyrrole using flow reactor [8]. The influence of temperature, equivalence ratio, and the presence of NO on the concentrations of CO, CO_2, HCN, and NO was analyzed. They pointed out that HCN was the only appreciable intermediate during pyrrole conversion.

In the present work, two low-pressure premixed pyrrole/O_2/Ar flames with equivalence ratios of 0.55 and 1.84 have been investigated with the currently developed molecular-beam mass spectrometry (MBMS) and tunable vacuum ultraviolet (VUV) synchrotron photoionization techniques [20–23]. Most flame species have been detected and identified by measurements of photoionization efficiency (PIE) spectra, and their mole fraction profiles have been determined as well. Furthermore, reaction pathways are proposed with particular attention to the major intermediates. Because of the important role that pyrrole plays in the combustion of coals, these data will be helpful in developing the kinetic model of pyrrole flames and extending the knowledge of the combustion chemistry of nitrogen-containing compounds.

2. Experimental methods

The experiments were performed at the flame endstation of the National Synchrotron Radiation Laboratory (NSRL), Hefei, China. The experimental setup has been reported elsewhere [22,24–28] and only a brief description is given here. The apparatus is composed of a flame chamber that contains a movable flat-flame burner (McKenna Burner) 6 cm in diameter, a differentially pumped chamber with a molecular-beam sampling system, and a photoionization chamber combined with a Reflectron time-of-flight mass spectrometer (RTOF-MS). Flame species are sampled by a quartz nozzle with a 40° included angle and an ~500-μm orifice at the tip. The sampled gas forms a molecular beam, which then passes into a differentially pumped ionization region through a nickel skimmer. The molecular beam is crossed with the tunable VUV synchrotron light in the photoionization chamber and the photoions are collected and analyzed by the RTOF-MS with an approximate mass resolution of 1400 [24]. Then the ion signals are amplified by a preamplifier (VT120C, ORTEC, USA) and recorded using a multiscaler (FAST Comtec P7888, Germany) with a bin width of 2 ns. A digital delay generator (DG535, USA) is used to trigger a pulsed power supply and the multiscaler as well.

A 1-m Seya-Namioka monochromator is used to disperse synchrotron radiation from a bending magnet beamline of the 800-MeV electron storage ring. The energy resolution $E/\Delta E$ (FWHM) is about 500 with average photon flux of about 5×10^{10} photons/s. A lithium fluoride (LiF) window with thickness 1.0 mm is used to eliminate higher-order harmonic radiation from the monochromator when the wavelength is longer than 105.0 nm. The photon flux is monitored by a silicon photodiode (SXUV-100) to normalize ion signals.

Pyrrole was purchased from Sinopharm Chemical Reagent Limited Co., Shanghai, China with a purity of $\geqslant$99.5%. No purification was carried out for this study. The experimental conditions of the two premixed flames are listed in Table 1. The equivalence ratio is calculated considering the following overall reaction of pyrrole oxidation:

$$C_4H_5N + 5.75O_2 \rightarrow 4CO_2 + NO + 2.5H_2O. \quad (1)$$

NO is considered as the final NO_x product, since it is more stable than NO_2 at high temperatures. Flow rates of O_2 and Ar are controlled by MKS mass flow controllers and flow rate of pyrrole is controlled by a syringe pump (ISCO 1000D, USA). Flame temper-

Table 1
Parameters of the investigated pyrrole flames

Flame	Rich flame	Lean flame
Equivalence ratio (ϕ)	1.84	0.55
Ratio of C/O/N	1:1.56:0.25	1:5.19:0.25
Dilution of Ar (%)	46	40.84
Cold gas velocity (cm s^{-1})	35.05	61.43
Pressure (Torr)	25	25
Flow rate of O_2 (SLM)	0.8	1.85
Flow rate of Ar (SLM)	0.9	1.4
Flow rate of pyrrole (ml min^{-1})	0.79	0.55

ature is measured with a 0.076-mm-diameter Pt/Pt–13% Rh thermocouple coated with an Y_2O_3–BeO anticatalytic ceramic to reduce catalytic effects [29].

A series of mass spectra are measured with the variation of photon energy at the fixed burner position. The integrated ion intensities for a specified mass are normalized by the photon flux and then plotted as a function of the photon energy, which yields PIE spectra containing precise information of ionization energies (IEs) of specific species. Considering the cooling effect of molecular beam, the experimental error for determining IE in this study is within 0.05 eV. Movement of the burner toward or away from the quartz nozzle allows the mass spectrum to be taken at different position in the flame. To avoid fragmentation of intermediates, mass spectra for calculating mole fractions are recorded near ionization thresholds. Thus, the following photon energies are selected for this study: 8.50, 9.00, 9.54, 10.00, 10.97, 11.81, and 16.53 eV. The mole fraction profiles are deduced with a method described by Cool et al. [30] with an uncertainty of ±25% for stable species and a factor of 2 for free radicals.

3. Results

3.1. Photoionization mass spectrometry

Fig. 1 displays the photoionization mass spectra of the rich and lean pyrrole flames at a photon energy of 11.81 eV (105.0 nm) with sampling positions 7.0 and 4.0 mm, respectively. The relative ion signals are amplified for different mass regions to clearly reveal the weak peaks. As can be seen from the figure, a series of peaks ranging from $m/e = 15$ to 120 can be observed. These peaks correspond to hydrocarbons, oxygenated and nitrogenous species, which may be combustion intermediates or fragment ions from photoionization. The strongest ion signal ($m/e = 67$) comes from pyrrole itself because the fuel is not consumed completely at the sampling position.

It is obvious that the mass spectra of the two flames are quite different. For example, the ion intensity ratio of $I(m/e = 26)/I(m/e = 30)$ in the rich flame is much higher than that detected in the lean flame. Furthermore, some peaks are observed only in the rich flame, for example, $m/e = 50$, 77, 91, and 103. In contrast, $m/e = 45$, 46, 57, and 99 can be detected only in the lean flame. There are many possible isomers for each mass and the total number of isomers increases rapidly with the increase of molecular weight. Thus, identification of these isomeric intermediates by measurements of PIE spectra is required.

3.2. Identification of flame species

In this study, about 60 intermediates in the rich flame and 50 intermediates in the lean flame are detected and identified, which are listed in Table 2 along

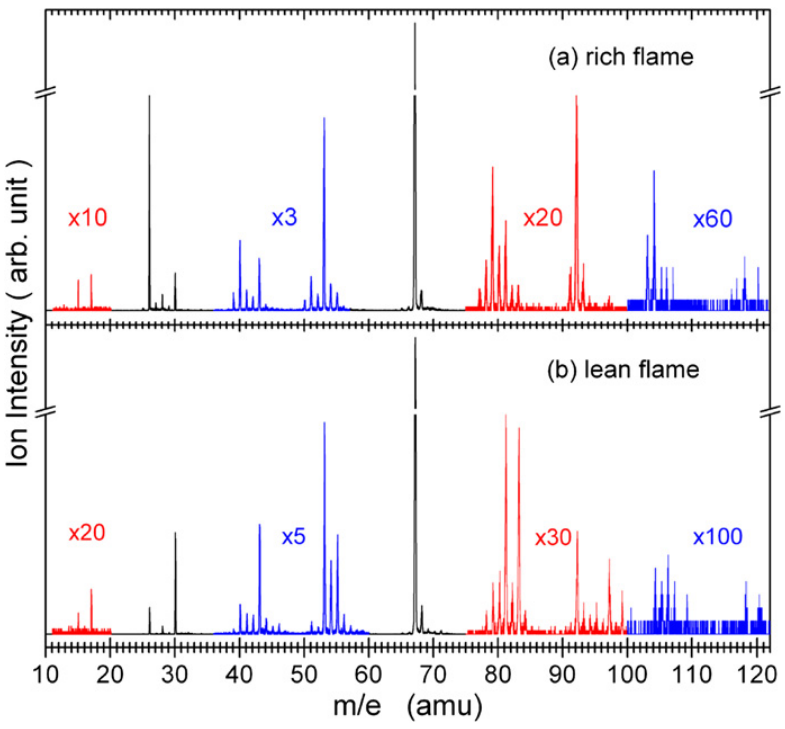

Fig. 1. Photoionization mass spectra of the rich and the lean pyrrole flames at the pressure of 25.0 Torr and the photon energy of 11.80 eV, taken at the sampling nozzle positions of 7.0 mm and 4.0 mm from the burner surface, respectively.

Table 2
Combustion intermediates measured with their respective IEs, maximum mole fractions (X_{max}), and positions in the fuel-rich and fuel-lean pyrrole fames

m/e	Formula	Species	IEs (eV)			Mole fractions			
			Literature[a]	This work[b]		Position (mm)		X_{max}	
				Rich	Lean	Rich	Lean	Rich	Lean
15	CH_3	methyl radical	9.84	9.82	9.81	8.5	5.5	6.72E−4	1.41E−4
17	NH_3	ammonia	10.2	10.20	10.22		5.5		4.76E−4
26	C_2H_2	acetylene	11.40	11.35	11.39	7.5	5.5	1.50E−2	5.67E−3
27	HCN	hydrogen cyanide	13.6	–	–	8.0	4.5	9.88E−2	9.81E−3
28	C_2H_4	ethylene	10.51	10.51	10.51	7.0	5.5	8.83E−4	1.94E−3
	N_2	nitrogen	15.58	–	–	–	6.0	–	1.94E−2
29	CH_3N	methanimine	9.97	9.99	10.03	6.0	5.0	1.02E−4	9.73E−5
30	NO	nitric oxide	9.26	9.26	9.26	–	–	–	–
	CH_2O	formaldehyde	10.86	10.85	10.86	–	–	–	–
32	CH_3OH	methanol	10.84	10.85	10.84	–	6.0	<1.0E−6	1.20E−3
39	C_3H_3	propargyl radical	8.67	8.68	8.67	8.5	5.5	2.05E−4	2.04E−5
40	C_3H_4	allene	9.83	9.84	9.85	8.0	5.0	4.70E−5	1.17E−4
		propyne	10.36	10.31	10.35	7.5	5.0	5.71E−4	
41	C_3H_5	allyl radical	8.18	8.17	8.18	8.5	3.5	4.56E−4	2.39E−5
	C_2H_3N	methyl isonitrile	11.24	11.23	11.26	7.0	5.0	7.73E−5	3.77E−4
42	C_2H_2O	ketene	9.62	9.61	9.61	8.0	5.5	2.97E−4	4.57E−4
43	C_3H_7	*n*-propyl radical	8.09	8.11	8.10	–	–	<1.0E−6	<1.0E−6
	HNCO	isocyanic acid	11.60	11.58	11.60	8.5	5.5	3.72E−3	1.04E−2
44[c]	C_2H_4O	ethenol	9.33	9.32	9.33	–	5.5	<1.0E−6	3.43E−4
		acetaldehyde	10.23	10.23	10.25				
45	CH_3NO	formamide	10.5	–	10.47	–	5.5	–	2.86E−4
46	CH_2O_2	formic acid	11.33	–	11.33	–	–	–	<1.0E−6
50	C_4H_2	1,3-butadiyne	10.17	10.18	–	8.5	–	6.72E−4	–
51[c]	C_3HN	isocyanoacetylene	11.23	–	11.16	–	5.5	–	2.80E−4
		propiolonitrile	11.62	11.58	11.63	8.5		2.80E−3	
52	C_4H_4	vinylacetylene	9.58	9.58	9.62	8.5	5.5	4.02E−5	7.29E−5
53	C_3H_3N	2-propenenitrile	10.91	10.90	10.90	8.5	5.5	1.05E−2	9.24E−3
54	C_4H_6	1,3-butadiene	9.07	9.07	–	5.5	–	6.32E−5	–
		1,2-butadiene	9.33	–	9.33	–	3.0	–	2.42E−5
55	C_3H_5N	2-propen-1-imine	9.65	9.65	9.65	7.0	5.0	8.33E−5	1.08E−4
56[c]	$C_2H_4N_2$	2,3-diazabutadiene	8.95	9.00	8.95	7.0	5.5	8.24E−5	1.64E−5
57	C_4H_9	isobutyl radical	7.93	–	7.93	–	4.0	–	1.37E−5
65[c]	C_5H_5	cyclopentadienyl radical	8.41	8.38	8.40	–	6.0	–	1.40E−4
	C_4H_3N	cyanoallene	10.35	10.38	10.34				
78	C_6H_6	benzene	9.24	9.24	9.25	6.5	6.0	2.11E−5	2.82E−5
79	C_5H_5N	pyridine	9.26	9.26	9.30	7.5	6.0	1.52E−4	1.75E−4
80	C_6H_8	1-hexen-3-yne	8.91	8.96	8.94	6.0	3.0	8.89E−5	7.23E−6
81	C_5H_7N	2-methylpyrrole	7.78	7.78	7.81	6.5	4.5	2.14E−4	3.65E−5
82	C_6H_{10}	1,3-hexadiene	8.54	8.56	–	6.5	–	2.25E−5	–
	C_5H_6O	2-methylfuran	8.58						
		2-pentyn-4-one	9.76	–	9.77	–	4.5	–	5.97E−5
83	C_6H_{11}	cyclohexyl radical	7.66	7.66	7.66	6.5	4.5	2.65E−4	1.12E−5
	C_5H_9N	1,2,3,6-tetrahydropyridine	8.64	8.73	8.63		3.0		1.55E−4
91	C_6H_5N	phenylnitrene	8.0[d]	8.02	–	7.0	–	5.13E−5	–
92	C_7H_8	toluene	8.85	8.87	8.87	8.0	5.0	2.58E−4	3.17E−5
93	C_6H_7N	aniline	7.72	7.74	7.76	7.0	4.0	1.53E−5	2.26E−6
	C_6H_5O	phenoxy radical	8.84	8.90	8.88	6.5	4.0	2.55E−5	4.67E−6
95[c]	C_6H_9N	2,5-dimethylpyrrole	7.69	7.75	7.75	6.0	3.5	1.54E−5	7.0E−6
	C_5H_5NO	2-pyridinol	8.62	8.60	8.60				
97	$C_6H_{11}N$	diallylamine	8.2	8.28	8.20	6.5	4.0	4.14E−5	8.95E−6
	C_5H_7NO	2,4-dimethyloxazole	9.34	–	9.37	–	3.5	–	5.42E−6
99	$C_6H_{13}N$	cyclohexanamine	8.86	–	8.84	–	4.5	–	3.18E−6
103	C_7H_5N	benzonitrile	9.71	9.70	–	8.0	–	2.09E−5	–

Table 2 (*continued*)

m/*e*	Formula	Species	IEs (eV)			Mole fractions			
			Literature[a]	This work[b]		Position (mm)		X_{max}	
				Rich	Lean	Rich	Lean	Rich	Lean
104	$C_6H_4N_2$	3-pyridinecarbonitrile	10.10	10.01	10.06	7.5	4.5	2.63E−5	2.60E−5
105[c]	C_8H_9	4-methylbenzyl radical	7.46	7.46	–	7.0	–	9.43E−6	–
	C_7H_7N	2-vinylpyridine	8.92	8.91					
	C_7H_7N	*N*-phenylmethanimine	8.73	–	8.72	–	4.0	–	4.46E−5
106	C_8H_{10}	*p*-xylene	8.44	8.41	8.40	7.0	4.0	2.41E−5	1.18E−5
107	C_7H_9N	*p*-toluidine	7.78	7.74	7.78	6.5	4.5	2.89E−5	4.12E−6
109	C_6H_7NO	6-methyl-2-pyridinol	8.33	–	8.29	–	–	–	<1.0E−6
116[c]	$C_6H_{16}N_2$	1,2-dipropylhydrazine	8.62	8.64	–	–	–	<1.0E−6	–
	C_9H_8	3-methylphenylacetylene	8.63						
117[c]	C_8H_7N	indolizine	7.26	7.41	–	7.5	–	1.50E−5	–
		m-tolunitrile	9.66	9.68					
118[c]	C_9H_{10}	1-phenylpropene	8.28	8.26	8.25	6.5	–	1.77E−5	<1.0E−6
		α-methylstyrene	8.3						
120	C_9H_{12}	3,3-dimethyl-6-methylene-1,4-cyclohexadiene	8.0	7.98	–	6.5	–	1.79E−5	–
		1,2,3-trimethylbenzene	8.42	–	8.42	–	3.5	–	7.33E−6

[a] Refers to [31] except for specific description.

[b] Errors for stable species are ±0.05 eV, for radicals are is ±0.10 eV.

[c] The values are the total mole fraction of a specific mass; for example, the mole fraction of 3.43E−4 for mass 44 includes both ethenol and acetaldehyde in the lean flame.

[d] Refers to [49].

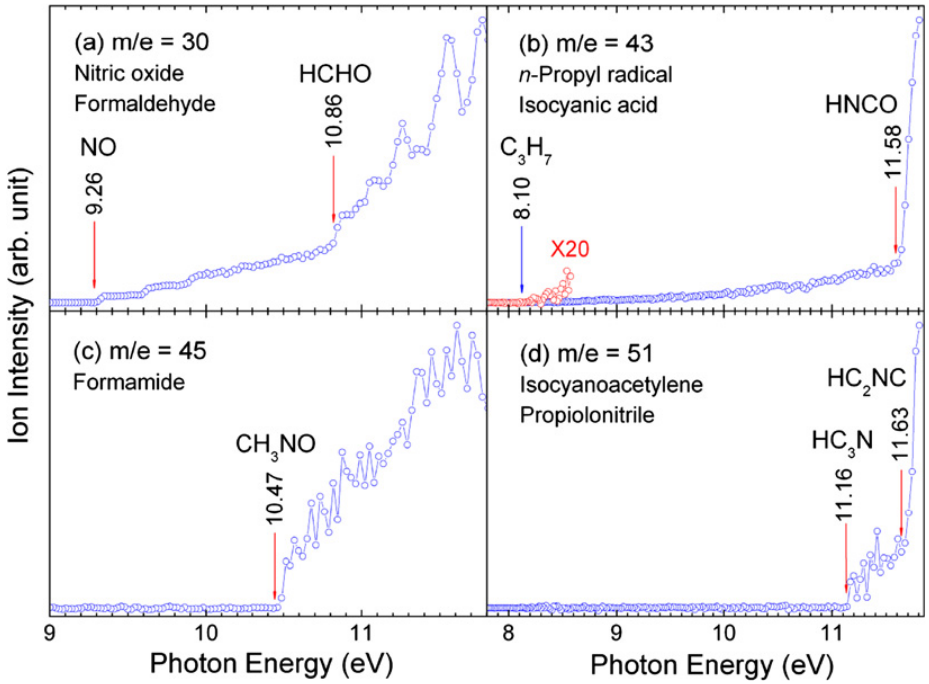

Fig. 2. The PIE spectra of (a) $m/e = 30$ (NO/HCHO), (b) $m/e = 43$ (C_3H_7/HNCO), (c) $m/e = 45$ (CH_3NO), and $m/e = 51$ (C_3HN) measured from the premixed fuel-lean pyrrole/O_2/Ar flame at a sampling nozzle position of 4.0 mm from the burner surface.

with literature IEs [31]. Some PIE spectra are selected for illustration here.

Fig. 2 displays PIE spectra of $m/e = 30$, 43, 45, and 51 observed in the lean flame. As shown in Fig. 2a, two onsets are observed at 9.26 and 10.86 eV for $m/e = 30$, which correspond to IEs of nitric oxide (NO, IE = 9.26 eV [31]) and formaldehyde (HCHO, IE = 10.86 eV [31]), respectively. This implies that NO and HCHO are formed in the lean flame. Two onsets are observed at 8.10 and 11.58 eV for $m/e = 43$, as indicated in Fig. 2b. These two onsets correspond to ionizations of the *n*-propyl radical (*n*-C_3H_7,

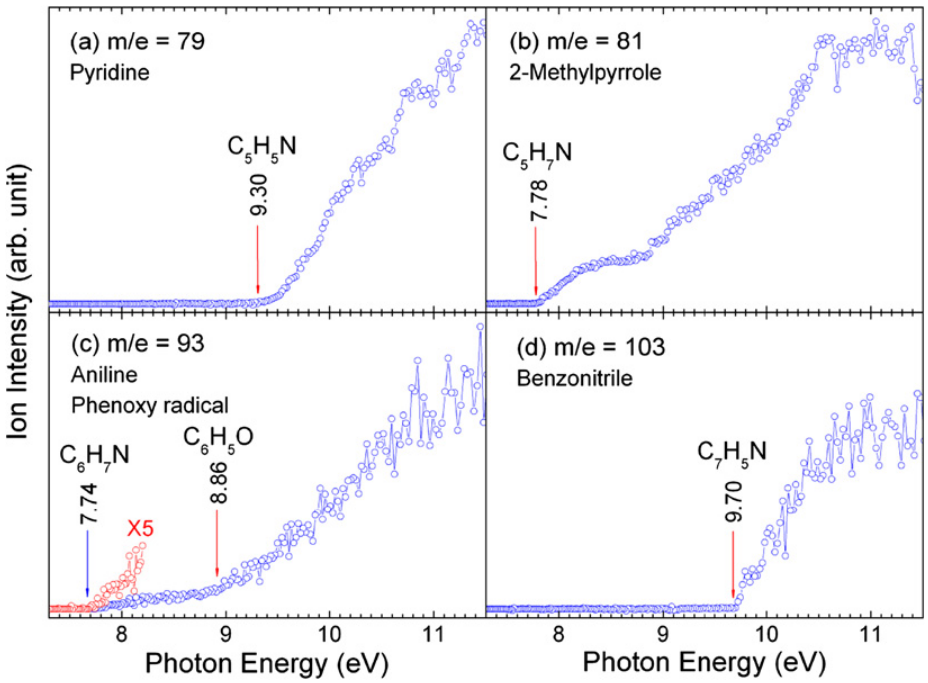

Fig. 3. The PIE spectra of (a) $m/e = 79$ (C_5H_5N), (b) $m/e = 81$ (C_5H_7N), (c) $m/e = 93$ (C_6H_7N/C_6H_5O), and $m/e = 103$ (C_7H_5N) measured from the premixed fuel-rich pyrrole/O_2/Ar flame at a sampling nozzle position 7.0 mm from the burner surface.

IE = 8.09 eV [31]) and isocyanic acid (HNCO, IE = 11.595 eV [31]), respectively. As an important intermediate for NO formation, HNCO is believed to be significant in combustion process of pyrrole. The n-C_3H_7 radical has not been reported previously either in thermal decomposition or in oxidation research on nitrogen-containing compounds. As shown in Fig. 2c, an onset at 10.47 eV is clearly observed in PIE spectra of $m/e = 45$, corresponding to ionization of formamide (IE = 10.5 eV [31]), which has never been observed in nitrogenous compound flames either. For mass 51, two onsets at 11.16 and 11.63 eV are observed in Fig. 2d, which are attributed to ionization thresholds of isocyanoacetylene (HCCNC, IE = 11.23 eV [31]) and propiolonitrile (HCCCN, IE = 11.62 eV [31]), respectively.

Fig. 3 shows four PIE spectra of radicals and stable intermediates observed in the rich flame. An onset at 9.30 eV is observed from the PIE spectra of $m/e = 79$, as shown in Fig. 3a, which is in agreement with IE of pyridine (IE = 9.26 eV [31]). Pyridine may be formed through the following reaction sequence: pyrrole ↔ pyrrolyl radical ↔ pyridoxy radical ↔ *ortho*-pyridinyl radical ↔ pyridine [32]. Besides this path, we suggest that the reactions of $C_3H_3N + C_2H_2$ and/or C_4H_4 + HCN could contribute to its formation. Fig. 3b shows PIE spectra of $m/e = 81$ with a clear onset at 7.78 eV. This value is in excellent accordance with the IE of 2-methylpyrrole (C_5H_7N), which has not been observed in previous oxidation studies of pyrrole [8]. PIE spectra of $m/e = 93$, as shown in Fig. 3c, indicate the presence of aniline (C_6H_7N) and the phenoxy radical (C_6H_5O) in the rich flame. Similarly, an onset is observed at 9.70 eV from the PIE spectra of $m/e = 103$ in Fig. 3d. This onset corresponds to ionization of benzonitrile (C_7H_5N, IE = 9.71 eV [31]). Besides the phenoxy, other radicals such as CH_3, C_2H_2N, C_3H_3, C_3H_5, C_3H_7, C_5H_5, C_6H_{11}, and C_8H_9 are observed in the rich flame as well.

Table 2 lists all observed flame species, from which we can see that some intermediates are detected in both the rich and lean flames, including CH_3, HCN, C_2H_2, HNCO, HCCCN, and 2-propenenitrile (C_3H_3N). However, some intermediates and radicals can be detected only in the rich flame, for instance, 1,3-butadiyne (C_4H_2), 1,3-butadiene (C_4H_6), 1,3-hexadiene (C_6H_{10}), 2-methylfuran (C_5H_6O), phenylnitrene (C_6H_5N), benzonitrile (C_7H_5N), 4-methylbenzyl radical (C_8H_9), 2-vinylpyridine (C_7H_7N), and indolizine/*m*-tolunitrile (C_8H_7N). On the other hand, formamide (CH_3NO), formic acid (CH_2O_2), 1,2-butadiene (C_4H_6), isobutyl radical (C_4H_9), 2-pentyn-4-one (C_5H_6O), 1,2,3,6-tetrahydropyridine (C_5H_9N), 2,4-dimethyloxazole (C_5H_7NO), cyclohexanamine ($C_6H_{13}N$), and *N*-phenyl methanimine (C_7H_7N), are observed only in the lean flame.

3.3. Mole fractions and temperature profiles

The mole fraction of each species is derived according to the method described by Cool et al. [30] and the data of the photoionization cross section. However, photoionization cross-section data on some

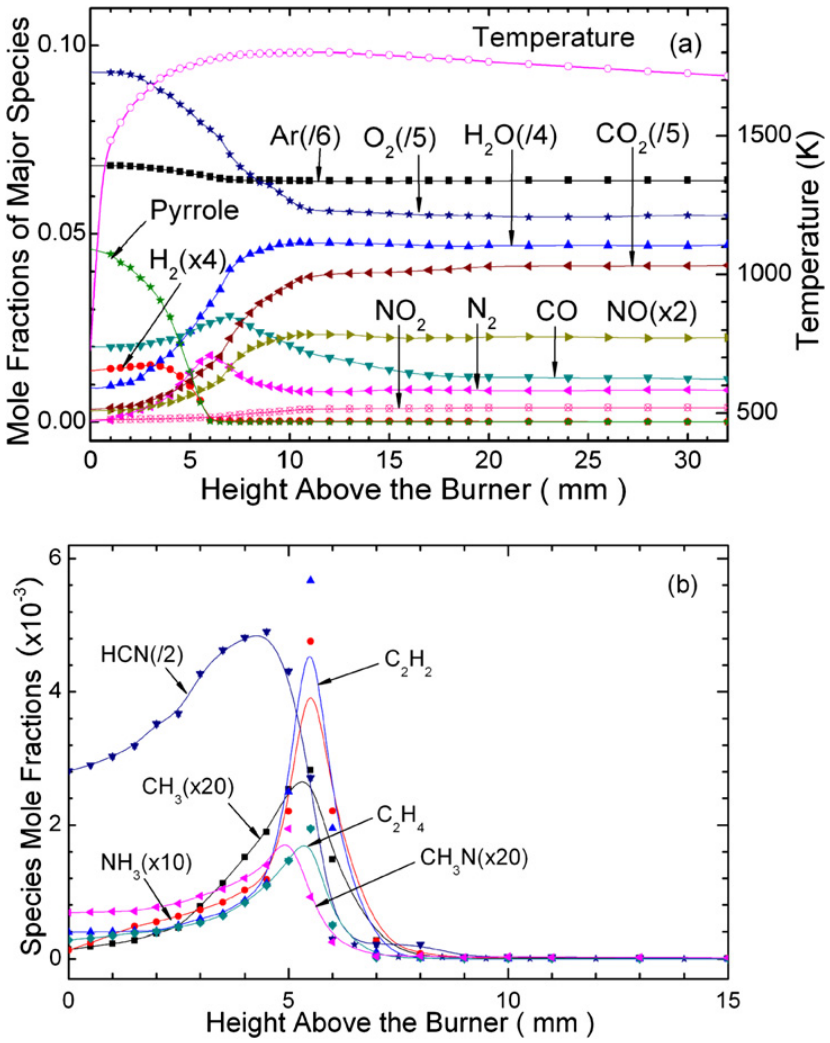

Fig. 4. (a) Mole fraction profiles of major species C_4H_5N, O_2, CO, CO_2, NO, N_2, NO_2, H_2O, H_2, and Ar, and the temperature profile measured from the lean flame. (b) Mole fraction profiles of CH_3, NH_3, C_2H_2, HCN, C_2H_4, and CH_3N measured from the lean flame.

flame species are not available, especially for nitrogenous intermediates. An estimated value of 5–10 Mb is used for these species when the photon energy is 0.5–1.0 eV higher than the specific IEs. Thus, mole fractions of these species may have larger uncertainties. The mole fractions of all observed species are calculated and the maximum values are listed in Table 2, along with their positions from the burner surface. The mole fraction profiles are shown in Figs. 4–7 for the lean flame and Figs. 8–11 for the rich flame. Symbols are experimental data and B-spline curves are used to guide the eye and extrapolate the data to 0 mm.

3.3.1. The lean pyrrole flame

The mole fraction profiles of the major species in the lean flame are displayed in Fig. 4a, along with the temperature profile. NO, N_2, and NO_2 are the major nitrogenous products in the postflame zone. The mole fraction of N_2 increases quickly to its maximum value of 0.0177 at 6 mm and then decreases to 0.008 at 32 mm. This is due to N_2 being converted from HCN rapidly under lean conditions and partly consumed by oxygen to form NO and NO_2. Besides these nitrogenous species, the other species are observed to be O_2, H_2O, CO, and CO_2 in the postflame zone. CO has the same tendency as N_2. The mole fraction of Ar decreases from 0.41 in the fresh gas to 0.38 in the postflame zone, which is used as a criterion to calculate the instrumental sampling function. The temperature attains 1530 ± 100 K at 1.0 mm. The maximum temperature is 1836 ± 100 K at 12.0 mm.

Fig. 4b shows the mole fraction profiles of CH_3, NH_3, C_2H_2, HCN, C_2H_4, and CH_3N. The methyl radical, the smallest hydrocarbon species detected in this flame, has a maximum mole fraction of 1.41×10^{-4} at 5.5 mm. It was thought to be formed from the reaction of hydrogen atom and C_3H_5CN [7,19] or through the path of acetylene and hydroxyl radical. Ammonia is an intermediate species in the lean flame with a maximum mole fraction of 4.76×10^{-4} at 5.5 mm. The oxidation of ammonia in flames has

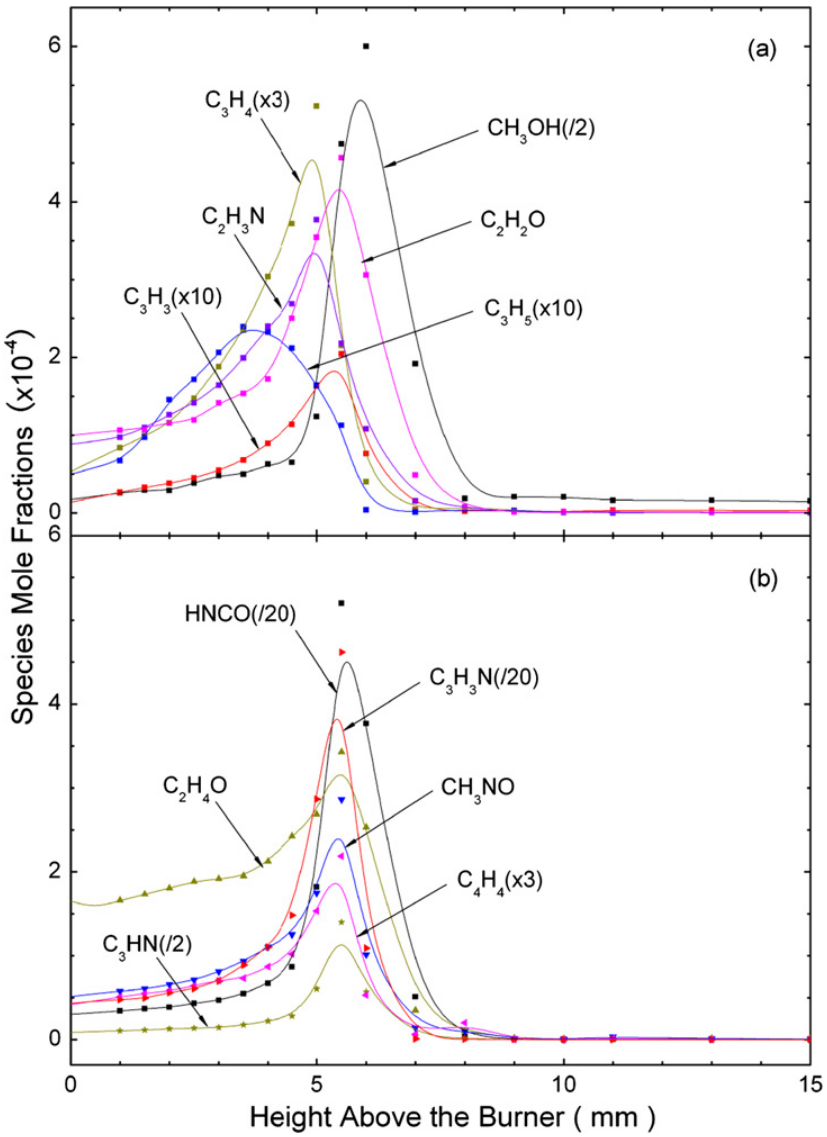

Fig. 5. (a) Mole fraction profiles of CH_3OH, C_3H_3, C_3H_4, C_3H_5, C_2H_3N, and C_2H_2O measured from the lean flame. (b) Mole fraction profiles of HNCO, C_2H_4O, CH_3NO, C_3HN, C_4H_4, and C_3H_3N measured from the lean flame.

been studied previously by Miller et al. [33] as well as other researchers [34–36]. They proposed that ammonia is mainly converted to N_2 and NO by reacting with O and OH, both of which are luxuriant in the lean flame. C_2H_2 and C_2H_4 are also detected in the flame and their mole fraction profiles are presented in Fig. 4b, which can convert to each other according to Martoprawiro et al.'s study [7]. The formation pathway of C_2H_2 could be a bond-cleavage reaction via a biradical formed through a ring open process, as suggested by Mackie et al. [19]. Ancia et al. suggested that C_2H_2 could be consumed by O and/or OH in the preflame zone [37]. Two main channels of the reaction of C_2H_2 with OH will produce CH_3 + CO and CH_2CO + H. The maximum mole fraction of HCN in the lean flame is 9.81×10^{-3}, indicating that HCN is an important intermediate in the lean flame. In addition, $m/e = 29$ is identified to be methanimine (CH_3N) and has a maximum mole fraction of 9.73×10^{-5} at 5 mm. It could be consumed by HCN, as suggested in the quantum mechanical studies of Roger et al. [38], forming 2,3-diazabutadiene ($C_2H_4N_2$), which is also identified in this flame.

Mole fraction profiles of CH_3OH, C_3H_3, a-C_3H_4/p-C_3H_4, C_3H_5, C_2H_3N, and C_2H_2O are displayed in Fig. 5a. Methanol has a maximum mole fraction of 1.20×10^{-3} at 6.0 mm and is thought to be formed from the radical recombination of CH_3 and OH. Propargyl radical (C_3H_3) is a common intermediate in hydrocarbon flames, and the same happens in pyrrole flames. The maximum mole fraction of C_3H_3 is 2.04×10^{-5} in the lean flame. Mackie et al. and Martoprawiro et al. suggested that C_3H_3 principally results from propyne and is mainly converted to benzene [7,19]. Allene (a-C_3H_4) is also identified in this flame. The onset at 10.38 eV in the PIE spectra of $m/e = 40$ could be attributed to propyne (p-C_3H_4, IE = 10.36 [31]). The total maxi-

mum mole fraction of mass 40 is 1.17×10^{-4}. Koger et al. thought that p-C_3H_4 is one of the most important products of the pyrrole decomposition [19]. However, they did not observe a-C_3H_4. Mass 41 includes the contributions of allyl radical (C_3H_5) and methyl isonitrile (CH_3NC) with maximum mole fractions of 2.39×10^{-5} and 3.77×10^{-4}, respectively. Mass 42 is attributed to ketene (C_2H_2O) according to the PIE spectra measurement. Ketene has a maximum mole fraction of 4.57×10^{-4} and could be formed through the reaction(s) of $C_2H_2 + O$ or/and $C_2H_3 + OH$ [37]. Since C_2H_3 has not been observed in this flame, we think that ketene is mainly produced from the former pathway.

Fig. 5b shows mole fraction profiles of HNCO, C_2H_4O, CH_3NO, C_3HN, C_4H_4, and C_3H_3N. HNCO is identified as isocyanic acid with a maximum mole fraction of 1.04×10^{-2}. HNCO, the simplest molecule containing the four dominant biogenic elements, carbon, hydrogen, nitrogen, and oxygen, is the initial decomposition product of cyanuric acid and the selective noncatalytic reducing agent of the Raprenox process for NO_x removal [39]. Spin-forbidden thermal dissociation of HNCO to the lowest energy products has been investigated in shock tubes by Mertens et al. [40] and Wu et al. [41]. Furthermore, HNCO is mainly consumed by reacting with O/OH and converted to NH and CO. n-C_3H_7 radical is observed in the lean flame with a maximum mole fraction less than 1.0×10^{-6}. Two isomers, ethenol and acetaldehyde (C_2H_4O), are confirmed to contribute to $m/e = 44$. The total maximum mole fraction of C_2H_4O is 3.43×10^{-4}. Ethenol has been found as a common intermediate in hydrocarbon flames [23]. Nitrous oxide is not measured in the present work because of the cutoff limitation of the LiF window. Mass 45 is identified to be formamide with a maximum mole fraction of 2.86×10^{-4}. Formamide is an important intermediate in the reaction between CH_3 and NO and it would convert to hydrogen cyanide based on the previous calculations of the potential energy diagram of CH_3NO [42]. Formic acid is identified in this flame with a maximum mole fraction less than 1×10^{-6}. Two isomers, HCCNC and HCCCN, have a total maximum mole fraction of 2.80×10^{-4}. The measurement of PIE spectra concludes that one species of $m/e = 53$ is 2-propenenitrile (C_3H_3N) with a maximum mole fraction of 9.24×10^{-3}. Furthermore, C_4H_4 is identified as vinylacetylene and has a peak mole fraction of 7.29×10^{-5} at 5.5 mm.

Mole fraction profiles of C_4H_6, C_3H_5N, C_2H_5NC, $C_2H_4N_2$, C_4H_9, and C_5H_5/C_4H_3N are presented in Fig. 6a. According to the PIE spectra of $m/e = 54$, an onset is observed clearly at 9.33 eV, which corresponds to ionization of 1,2-butadiene with a maximum mole fraction of 2.42×10^{-5}. An unclear onset at 9.8–9.9 eV is observed in the PIE spectra of $m/e = 54$ also, which implies that C_3H_4N could be formed through CH-elimination from the biradical C_4H_5N, which is formed after the ring open reaction. For $m/e = 55$, 2-propen-1-imine (C_3H_5N) is distinguished and its maximum mole fractions is 1.08×10^{-4}. Mass 56 may be composed of a nitrogen-containing intermediate, 2,3-diazabutadiene ($C_2H_4N_2$), with a maximum mole fraction of 1.64×10^{-5} at 5.5 mm. The formation channels of 2,3-diazabutadiene have been discussed above. C_4H_9, as displayed in Fig. 6a, is identified as the isobutyl radical with a maximum mole fraction of 1.37×10^{-5}. For $m/e = 65$, both the cyclopentadienyl radical (C_5H_5) and cyanoallene (C_4H_3N) are identified. The maximum mole fraction of C_5H_5 is less than 1.00×10^{-6} and C_4H_3N has a peak mole fraction of 1.40×10^{-4} at 6.0 mm.

Fig. 6b shows the mole fraction profiles of C_6H_6, C_5H_5N, C_6H_8, C_5H_7N, C_5H_6O, C_6H_{11}, and C_5H_9N. C_6H_6 is identified as benzene and has a maximum mole fraction of 2.82×10^{-5} at 6.0 mm. The formation pathways of benzene have been investigated in hydrocarbon flames [43]. However, its production has never been reported in oxidation studies of nitrogen-containing compounds. C_5H_5N corresponds to pyridine and has a maximum mole fraction of 1.75×10^{-4} at 6.0 mm. The measurement of PIE spectra indicates that both 1-hexen-3-yne (C_6H_8, $m/e = 80$) and 2-pentyn-4-one (C_5H_6O, $m/e = 82$) exist in the lean flame with peak mole fractions of 7.23×10^{-6} and 5.97×10^{-5}, respectively. An onset at 7.81 eV is observed clearly on the PIE spectra of $m/e = 81$, which suggests that 2-methylpyrrole (C_5H_7N, IE = 7.78 eV) is formed in this flame. 2-Methylpyrrole could be produced from the reaction of pyrrole and methyl radical and its maximum mole fraction is 3.65×10^{-5}. Cyclohexyl radical (C_6H_{11}) and 1,2,3,6-tetrahydropyridine (C_5H_9N), both being confirmed to contribute to $m/e = 83$, have maximum mole fractions of 1.12×10^{-5} and 1.55×10^{-4}, respectively.

The mole fraction profiles of species of C_7H_8, C_6H_7N, C_6H_5O, C_6H_9N/C_5H_5NO, $C_6H_{11}N$, C_5H_7NO, and $C_6H_{13}N$ are displayed in Fig. 7a. C_7H_8 is assigned to toluene with a maximum mole fraction of 3.17×10^{-5}. For $m/e = 93$, two species, phenoxy radical (C_6H_5O) and aniline (C_6H_7N) exist in the lean flame with maximum mole fractions of 4.67×10^{-6} and 2.26×10^{-6}, respectively. For $m/e = 95$, two species are identified to be 2,5-dimethylpyrrole (C_6H_9N) and 2-pyridinol (C_5H_5NO) with a total maximum mole fraction of 7.0×10^{-6} at 3.5 mm. 2,5-Dimethylpyrrole could be formed by the reaction of 2-methylpyrrole and methyl radical. 2-Pyridinol may be produced from pyridine and oxygen atom. Mass

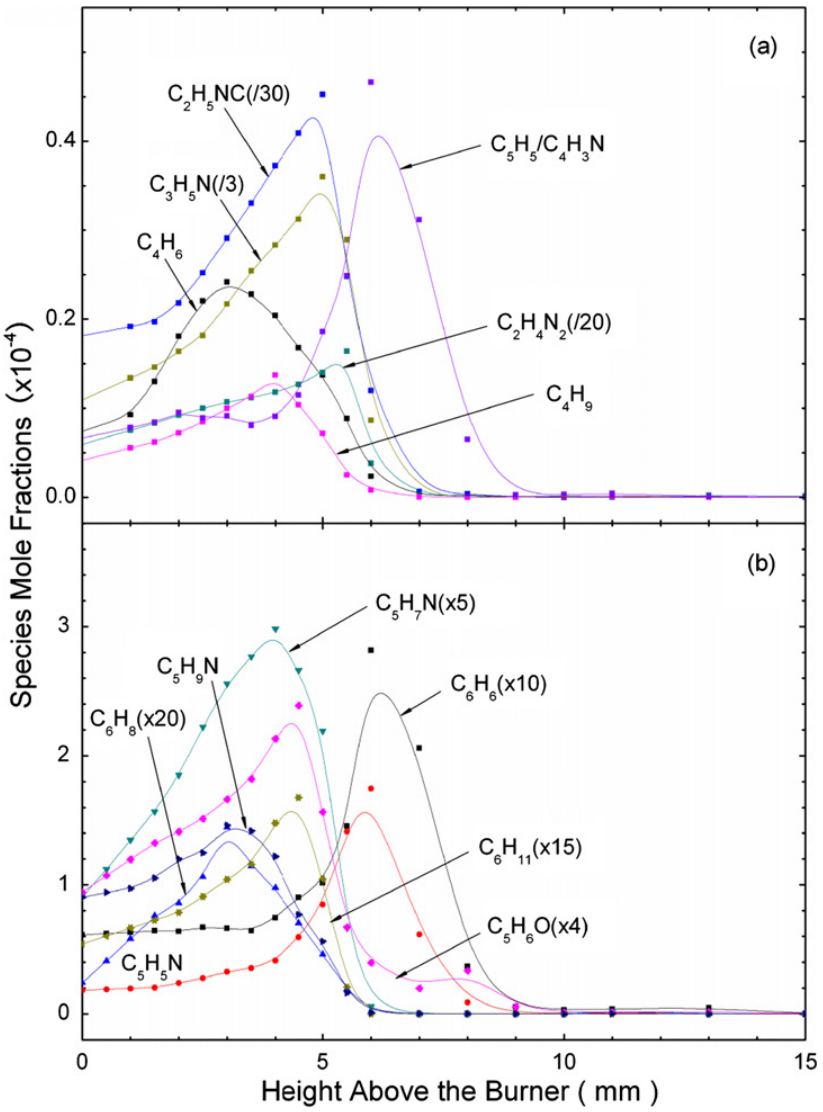

Fig. 6. (a) Mole fraction profiles of C_4H_6, C_3H_5N, C_2H_5NC, $C_2H_4N_2$, C_4H_9, and C_5H_5/C_4H_3N measured from the lean flame. (b) Mole fraction profiles of C_6H_6, C_5H_5N, C_6H_8, C_5H_7N, C_5H_6O, C_6H_{11}, and C_5H_9N measured from the lean flame.

97 is identified to be diallylamine ($C_6H_{11}N$) and 2,4-dimethyloxazole (C_5H_7NO) with maximum mole fractions of 8.95×10^{-6} and 5.42×10^{-6}, respectively. Furthermore, $C_6H_{13}N$ is identified to be cyclohexanamine with a peak mole fraction of 3.18×10^{-6} at 4.5 mm.

Fig. 7b shows mole fraction profiles of $C_6H_4N_2$, C_7H_7N, C_8H_{10}, C_7H_9N, and C_9H_{12}. $C_6H_4N_2$ is attributed to 3-pyridinecarbonitrile and has a maximum mole fraction of 2.60×10^{-5} at 4.5 mm. *N*-phenylmethanimine (C_7H_7N) is detected only in the lean flame and has a peak mole fraction of 4.46×10^{-5}. According to the measurement of PIE spectra, *p*-xylene (C_8H_{10}) and *p*-toluidine (C_7H_9N) are detected with peak mole fractions of 1.18×10^{-5} and 4.12×10^{-6}, respectively. C_6H_7NO is identified to be 6-methyl-2-pyridinol in the lean flame. Its peak mole fraction is less than 1.00×10^{-6}, whose profile is not shown in Fig. 7b. An onset at 8.25 eV is observed in the PIE spectra of $m/e =$ 118, which implies the presence of 1-phenylpropene and/or α-methylstyrene. Their total maximum mole fraction is less than 1×10^{-6}. Moreover, C_9H_{12} is assigned to 1,2,3-trimethylbenzene with a maximum mole fraction of 7.33×10^{-6} at 3.5 mm.

3.3.2. *The rich pyrrole flame*

Mole fraction profiles for the major species C_4H_5N, O_2, CO, CO_2, NO, N_2, NO_2, NH_3, H_2O, H_2, and Ar in the rich pyrrole flame are presented in Fig. 8a, along with the temperature profile. The reaction zone is located within 10 mm of the burner surface. It is obvious that NO, N_2, NO_2, and NH_3 are the dominating nitrogenous products, which is different from the lean flame. The mole fraction of Ar decreases from 0.46 in the fresh gas to 0.32 in the postflame zone. Pyrrole and O_2 are completely consumed at 9 and 14 mm, respectively. The flame temperature attains 945 ± 100 K at 1.0 mm and reaches

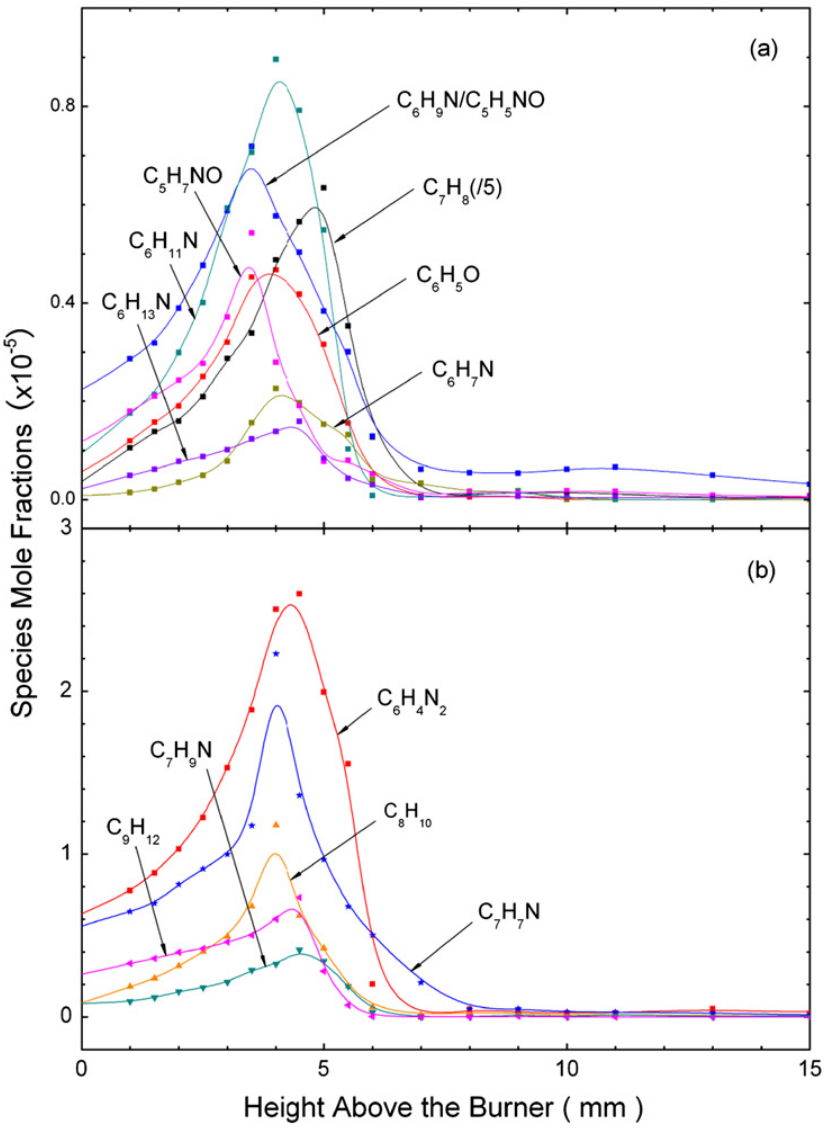

Fig. 7. (a) Mole fraction profiles of C_7H_8, C_6H_7N, C_6H_5O, C_6H_9N/C_5H_5NO, $C_6H_{11}N$, C_5H_7NO, and $C_6H_{13}N$ measured from the lean flame. (b) Mole fraction profiles of $C_6H_4N_2$, C_7H_7N, C_8H_{10}, C_7H_9N, and C_9H_{12} measured from the lean flame.

its maximum value of 1662 ± 100 K at 9.0 mm, which is about 170 K lower than that in the lean flame.

Fig. 8b shows the mole fraction profiles for species of CH_3, C_2H_2, HCN, C_2H_4, and CH_3N sampled from the rich pyrrole flame. The smallest hydrocarbon species measured in this flame is the methyl radical, with a maximum mole fraction of 6.72×10^{-4}. Methane and NH are not measured in this study because of the cutoff limitation of the LiF window. Two C_2-species, C_2H_2 and C_2H_4, are detected with maximum mole fractions of 1.50×10^{-2} and 8.83×10^{-4}, respectively. Vinyl and ethyl radicals are not observed in this flame, which is in agreement with previous study by Lumbreras et al. [8]. Previous studies revealed that the gas-phase fuel–nitrogen reaction sequence is initiated by a rapid and nearly quantitative conversion of the parent fuel nitrogen compounds to hydrogen cyanide and ammonia [44–46]. In this study, HCN has a maximum mole fraction of 9.88×10^{-2} and its presence results from thermal decomposition of pyrrole in the preflame zone. The PIE spectra of $m/e = 29$ show that there is an apparent onset at 9.99 eV, which is close to the IE (9.97 eV [47]) of methanimine (CH_3N). Therefore, $m/e = 29$ corresponds to methanimine with a maximum mole fraction of 1.02×10^{-4}, which has not been observed in previous studies of pyrrole oxidation.

Mole fraction profiles of C_3H_3, a-C_3H_4, p-C_3H_4, C_3H_5, C_2H_3N, C_2H_2O, and HNCO are displayed in Fig. 9a. The propargyl radical is identified in this flame with a maximum mole fraction of 2.05×10^{-4}, which is about 10 times that in the lean flame. The maximum mole fractions of a-C_3H_4 and p-C_3H_4 are 4.70×10^{-5} and 7.63×10^{-4}, respectively. Allyl radical (C_3H_5) and methyl isonitrile (C_2H_3N) with peak mole fractions of 4.56×10^{-4} and 1.13×10^{-5} are also detected in the rich flame, respectively. According to the kinetic model of pyrrole pyrolysis, C_3H_5

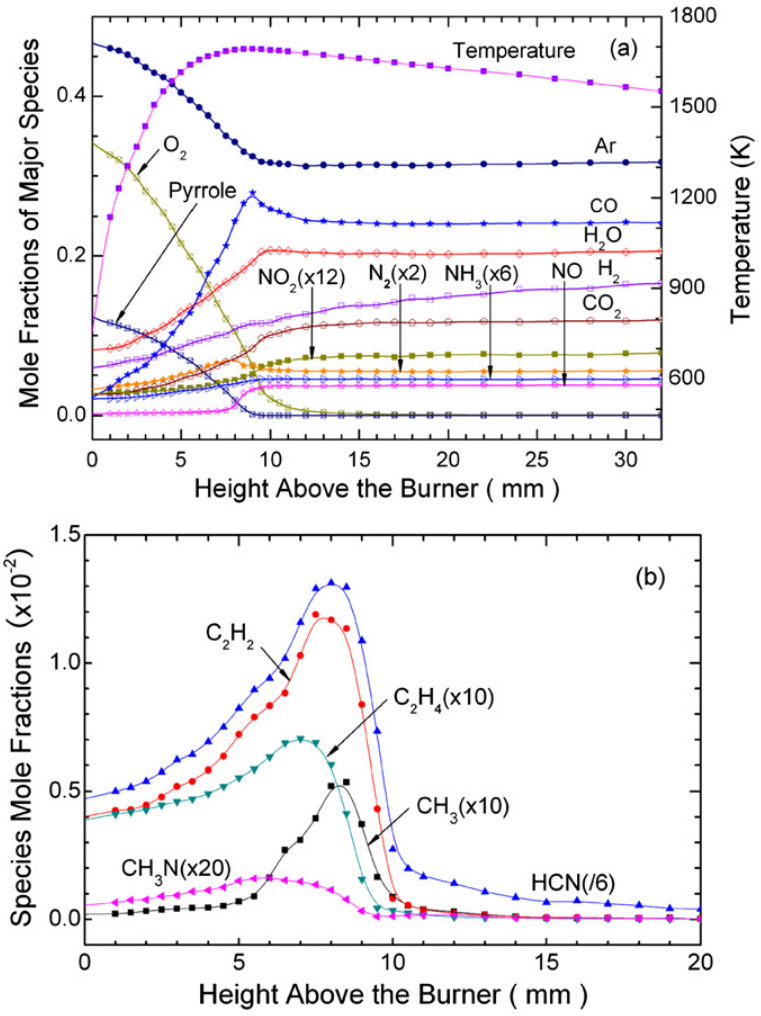

Fig. 8. (a) Mole fraction profiles of major species C_4H_5N, O_2, CO, CO_2, NO, N_2, NO_2, NH_3, H_2O, H_2, and Ar and the temperature profile measured from the rich flame. (b) Mole fraction profiles of $m/e = CH_3$, C_2H_2, HCN, C_2H_4, and CH_3N measured from the rich flame.

is produced from the reaction of H atom and allyl cyanide and can lose a hydrogen atom to produce allene/propyne [7]. The onset at 9.61 eV in PIE spectra of mass 42 is attributed to ketene. Its maximum mole fraction is 2.97×10^{-4}, which is about half of that in the lean flame. HNCO is also formed in the rich flame with its maximum mole fraction of 3.72×10^{-3}, which is about one-third of that in the lean flame. In addition, the n-C_3H_7 radical is the other observed intermediate for mass 43, with a low concentration, which we estimate to be less than 1×10^{-6}.

Fig. 9b shows the mole fraction profiles of C_4H_2, C_3HN, C_4H_4, C_3H_3N, C_4H_6, C_3H_5N, and $C_2H_4N_2$. Three C_4-species, 1,3-butadiyne (C_4H_2), vinylacetylene (C_4H_4), and 1,3-butadiene (C_4H_6), are detected with maximum mole fractions of 6.72×10^{-4}, 4.02×10^{-5}, and 6.32×10^{-5}, respectively. These species may be formed through the reactions (2)–(4) suggested by Mackie et al. [19]:

$$2C_2H_2 \leftrightarrow C_4H_4, \tag{2}$$

$$C_4H_4 \leftrightarrow H_2 + C_4H_2, \tag{3}$$

$$C_3H_5 + CH_2CN \leftrightarrow C_4H_6 + HCN. \tag{4}$$

HCCCN, C_3H_3N, and 2-propen-1-imine (C_3H_5N) are also detected and their maximum mole fractions are 2.80×10^{-3}, 1.05×10^{-2}, and 8.33×10^{-5}, respectively. For $m/e = 56$, 2,3-diazabutadiene ($C_2H_4N_2$) is identified with a maximum mole fraction of 8.24×10^{-5} at 7.0 mm.

Mole fraction profiles of C_6H_6, C_5H_5N, C_6H_8, C_5H_7N, C_5H_6O/C_6H_{10}, and C_6H_{11}/C_5H_9N are presented in Fig. 10a. Benzene is a minor intermediate in the rich flame. Its maximum mole fraction is 2.11×10^{-5}. Previous theoretical studies indicated that it can be produced from propargyl radical via a rudimentary pathway containing reactions (5) and (6) in the pyrolysis of pyrrole [7,19,48]:

$$2C_3H_3 \leftrightarrow \text{L-}C_6H_6, \tag{5}$$

$$\text{L-}C_6H_6 \leftrightarrow C_6H_6. \tag{6}$$

The reaction between benzene and H or O is one of the consumption pathways of benzene in the flame.

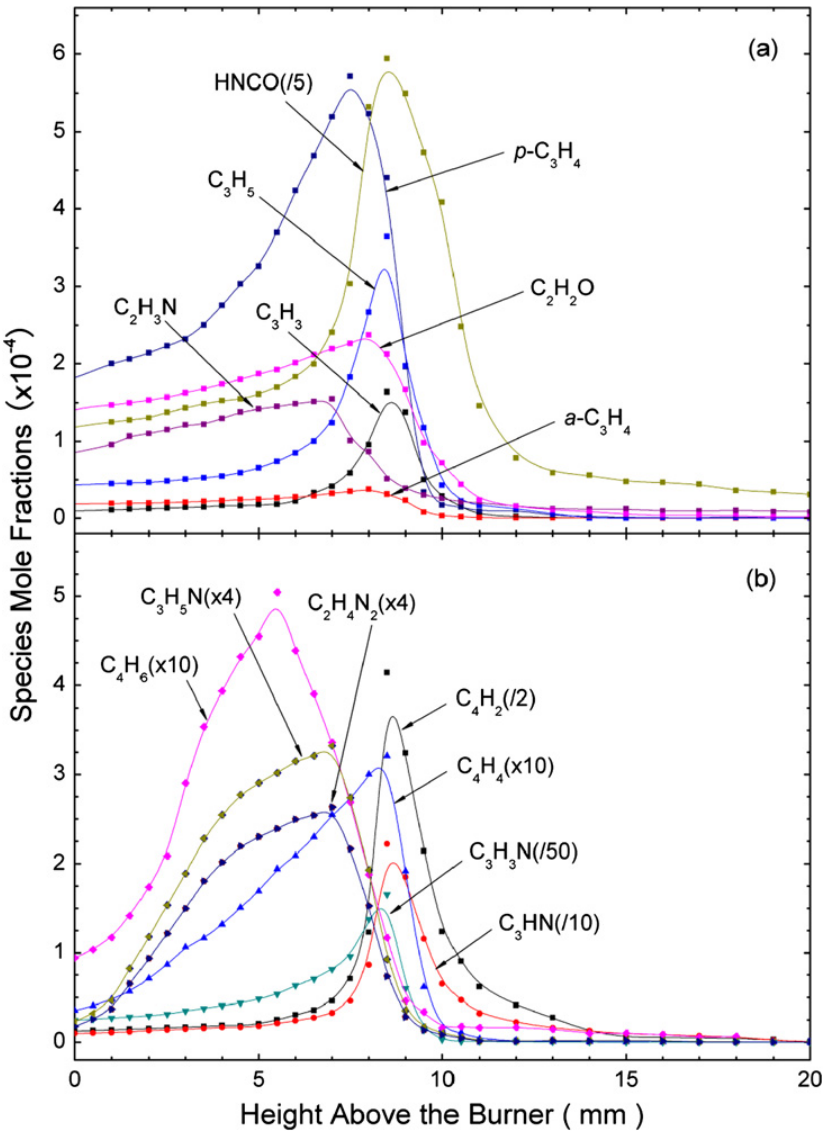

Fig. 9. (a) Mole fraction profiles of C_3H_3, C_3H_4 (allene), C_3H_4 (propyne), C_3H_5, C_2H_3N, C_2H_2O, and HNCO measured from the rich flame. (b) Mole fraction profiles of C_4H_2, C_3HN, C_4H_4, C_3H_3N, C_4H_6, C_3H_5N, and $C_2H_4N_2$ measured from the rich flame.

C_6H_8 is identified as 1-hexen-3-yne and has a maximum mole fraction of 8.89×10^{-5}. C_5H_5N and C_5H_7N are identified as pyridine and 2-methylpyrrole, with maximum mole fractions of 1.52×10^{-4} and 2.14×10^{-4}, respectively. Mass 82 may contain the contributions of 1,3-hexadiene (C_6H_{10}) and an oxygenated species 2-methylfuran (C_5H_6O) and has a total maximum mole fraction of 2.25×10^{-5}. Cyclohexyl radical (C_6H_{11}) and 1,2,3,6-tetrahydropyridine (C_5H_9N) are proved to contribute to mass 83 and have a total maximum mole fraction of 2.65×10^{-4}.

Fig. 10b displays the mole fraction profiles of C_6H_5N, C_7H_8, C_6H_5O, C_6H_7N, C_6H_9N/C_5H_5NO, and $C_6H_{11}N$. The onsets at 8.02 and 9.14 eV on the PIE spectra of mass 91 correspond to the rising points of the first and second peaks of photoelectron spectroscopy of phenylnitrene (PhN, C_6H_5N) in a previous study by Che et al. [49], which cannot be observed in the lean flame. PhN is a biradical because the two spin-parallel electrons occupy two different orbitals, $3b_1$ and $3b_2$. Its ground state is the triplet $^3A_2$ state. There have been some previous studies of PhN [49–56]. Its maximum mole fraction is 5.13×10^{-5} at 7.0 mm, presented in Fig. 10b. Toluene (C_7H_8, $m/e = 92$) is detected in the rich flame according to the PIE spectra. It has a peak mole fraction of 2.58×10^{-4} at 8.0 mm, which is about eight times higher than that in the lean flame. Riedl et al. indicated that toluene can be formed from benzonitrile [57]. Mass 93 contains the contributions of phenoxy radical (C_6H_5O) and aniline (C_6H_7N) with maximum mole fractions of 4.68×10^{-5} at 6.5 mm and 2.30×10^{-5} at 7.0 mm, respectively. Phenoxy radical can be formed through the reaction of C_6H_5 and oxygen [58]. Similarly, mass 95 could be a mixture of 2,5-dimethylpyrrole (C_6H_9N) and 2-pyridinol (C_5H_5NO) with a peak value of 1.54×10^{-5}. Furthermore, $C_6H_{11}N$ is identified to be diallylamine with a

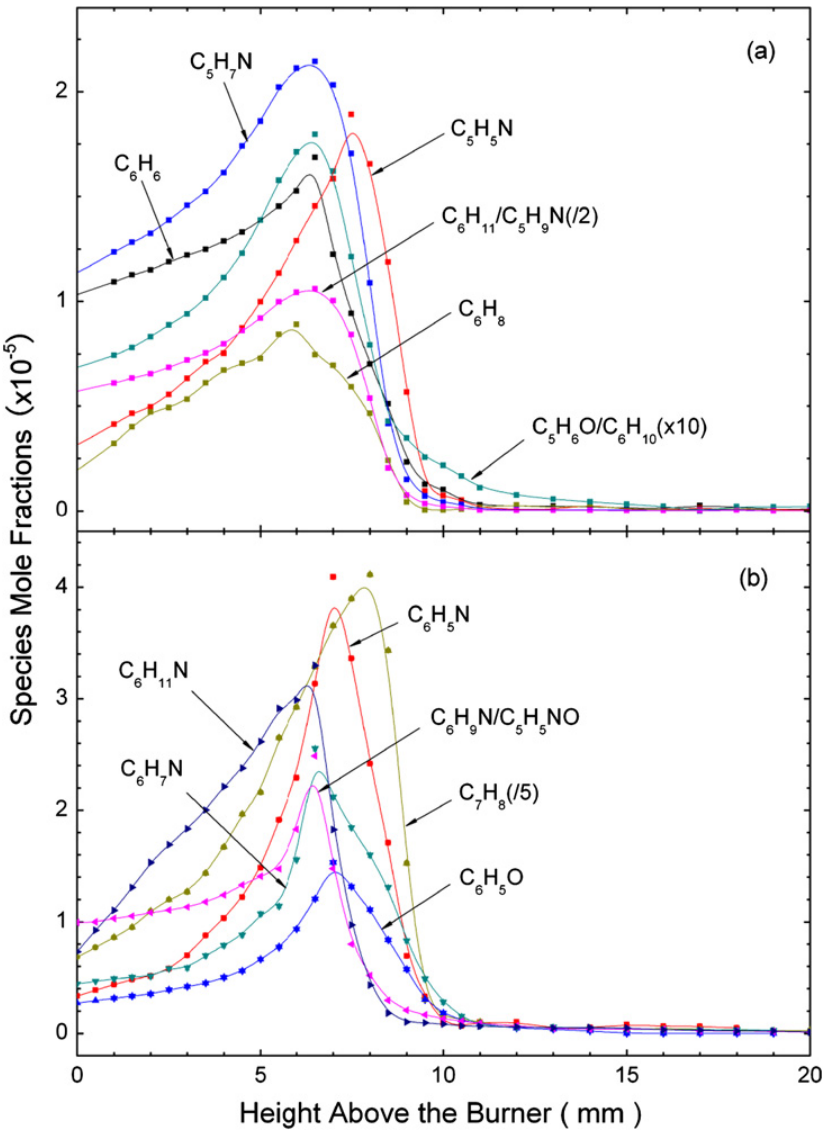

Fig. 10. (a) Mole fraction profiles of C_6H_6, C_5H_5N, C_6H_8, C_5H_7N, C_5H_6O/C_6H_{10}, and C_6H_{11}/C_5H_9N measured from the rich flame. (b) Mole fraction profiles of C_6H_5N, C_7H_8, C_6H_5O, C_6H_7N, C_6H_9N/C_5H_5NO, and $C_6H_{11}N$ measured from the rich flame.

maximum mole fraction of 4.14×10^{-5} at 6.5 mm, which can be formed by the reaction of C_3H_5N and C_3H_6.

Mole fraction profiles of C_7H_5N, $C_6H_4N_2$, C_8H_9/C_7H_7N, C_8H_{10}, and C_7H_9N are shown in Fig. 11a. In correspondence with PhN, benzonitrile (C_7H_5N) is observed only in the rich flame. Its maximum mole fraction is 2.09×10^{-5} at 8.0 mm and it can be produced from C_3HN and C_4H_4. As shown in Fig. 11a, the peak value of 3-pyridinecarbonitrile ($C_6H_4N_2$) is 2.63×10^{-5} at 7.5 mm. Mass 105 includes 4-methylbenzyl radical (C_8H_9) and 2-vinylpyridine (C_7H_7N) basing on the measurement of PIE spectra and has a total maximum mole fraction of 9.43×10^{-6}, which exists only in the rich flame. Furthermore, species of mass 106 is *p*-xylene (C_8H_{10}) and its maximum mole fraction is 2.41×10^{-5} at 7.0 mm. C_7H_9N ($m/e = 107$) can be identified to be *p*-toluidine with a peak mole fraction of 2.89×10^{-5}.

Fig. 11b shows the mole fraction profiles of C_8H_7N, C_9H_{10}, and C_9H_{12}. The heaviest nitrogen-containing intermediate identified in the rich flame is C_8H_7N, which contains the contributions of *m*-tolunitrile and indolizine, reaching a peak mole fraction of 1.50×10^{-5}. *m*-Tolunitrile could be formed from benzonitrile [57]. Mass 118 is assigned to 1-phenylpropene (C_9H_{10}) with a maximum mole fraction of 1.77×10^{-5} at 6.5 mm. C_9H_{12}, the heaviest species observed in the rich flame, is identified to be 3,3-dimethyl-6-methylidene-1,4-cyclohexadiene with a peak mole faction of 1.79×10^{-5} at 6.5 mm.

4. Discussion

There have been some previous investigations on the kinetics of pyrolysis of pyrrole [7,17,19,59–62]. The reaction pathways in the pyrrole flames proposed

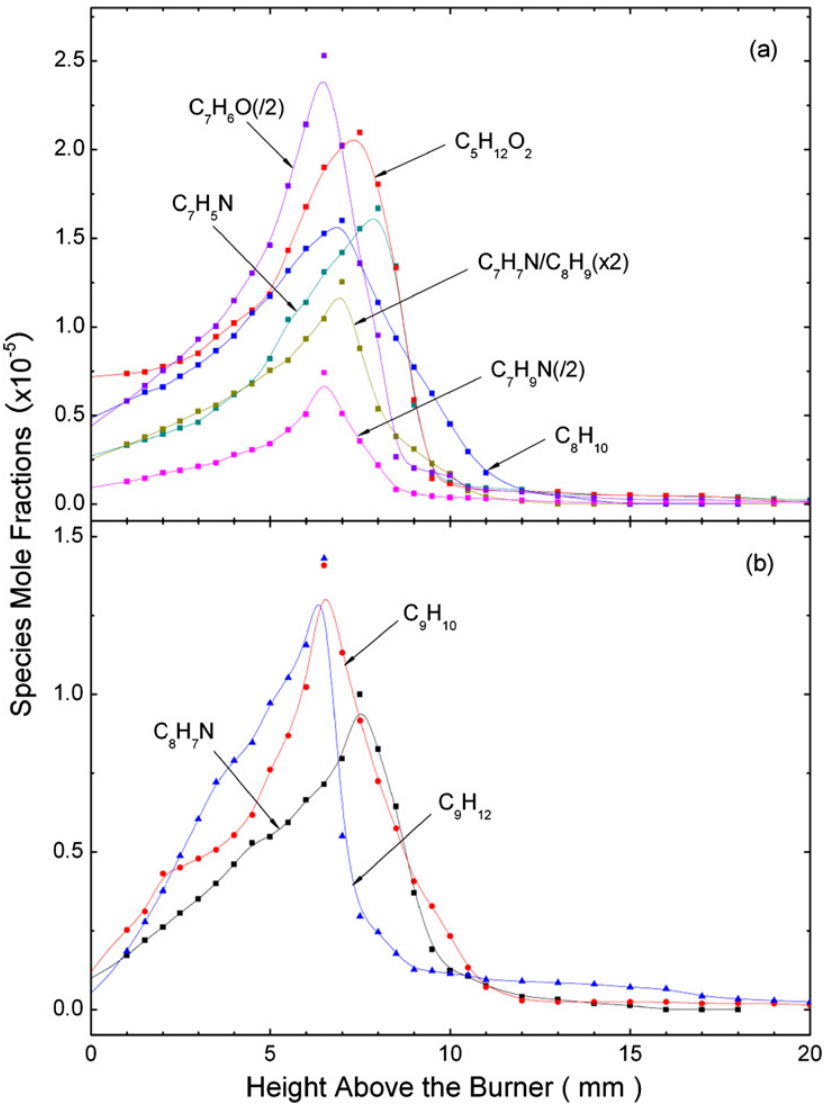

Fig. 11. (a) Mole fraction profiles of C_7H_5N, $C_6H_4N_2$, C_8H_9/C_7H_7N, C_8H_{10}, and C_7H_9N measured from the rich flame. (b) Mole fraction profiles of C_8H_7N, C_9H_{10}, and C_9H_{12} measured from the rich flame.

in the present study are mainly based on the results of Mackie et al. [19] and Martoprawiro et al. [7] for pyrrole pyrolysis, Doughty and Mackie [63] for butenenitrile pyrolysis, and the recent kinetic model of pyrrole oxidation by Lumbreras et al. [8].

Since the detailed modeling work of pyrrole flames remains absent, the discussion about the nitrogen conversion process is mainly deduced from the species identification and mole fraction calculation. Fig. 12 outlines schematically the principal reactions for the major intermediates and products. It is well known that pyrrole can suffer a thermal rearrangement at temperatures between 770 and 870 K [64], leading to the formation of pyrrolenine (2H-pyrrole, C_4H_5N), which presents both thermal and photochemical rearrangements of pyrrole [19]. This rearrangement is supported by theoretical researchers [7,60]. However, this species has not been detected in previous studies. As seen from the PIE spectra of $m/e = 67$, the onsets at 9.00 eV in the rich flame and 9.04 eV in the lean flame are in agreement with the IE of pyrrolenine (8.997 eV), which is calculated by the density functional B3LYP method using the 6-31G(d) basis set [65]. Therefore, the isomerization of pyrrole to produce pyrrolenine is validated to be the other initial pathway of its decomposition besides the hydrogen abstraction to produce pyrrolyl radical. On the one hand, the pyrrolyl radical is consumed by H/O/OH and mainly converted to C_3H_3, p-C_3H_4, HCN, and HNCO [19]. On the other hand, pyrrolenine may undergo isomerization to form methacrylonitrile, crotonitrile, and allyl cyanide or thermolysis to form biradicals by scission of the C–N bond, while reactions of pyrrolenine with the radicals appear to be less important [7,19,63]. Bacskay et al. had performed the potential energy surface calculation for the formation of HCN and p-C_3H_4 from thermal decomposition of pyrrole and concluded that the heat of the pyrrole → pyrrolenine → HCN + C_3H_4 reaction will lie below the observed activation

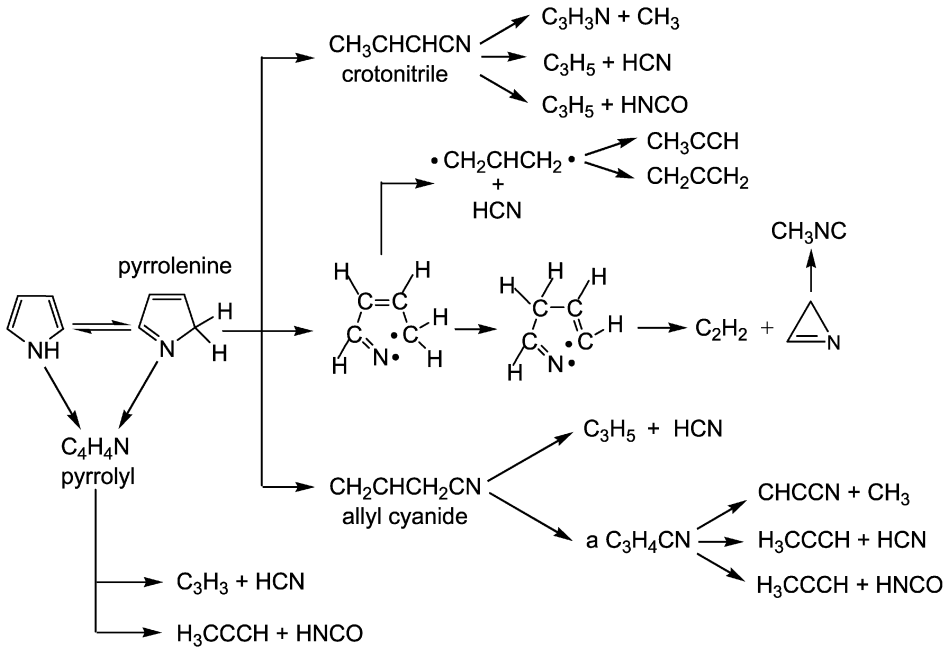

Fig. 12. Reaction path diagram illustrating the oxidation process of pyrrole in low-pressure premixed flames.

energy only if the product C_3H_4 is propyne, allene or cyclopropene [60], indicating that HCN and p-C_3H_4 can be produced from pyrrolenine.

Doughty and Mackie reported that the major primary products of pyrrole pyrolysis were straight isomers, allyl cyanide and crotonitrile. They could convert to each other easily via the reaction [63]

$$CH_3CHCHCN \leftrightarrow CH_2CHCH_2CN. \quad (7)$$

Crotonitrile can be isomerized to allyl cyanide quickly and dissociates into the CN and allyl radicals [66]. Therefore, we mainly take into account crotonitrile and allyl cyanide to demonstrate the reaction pathways of pyrrole in flames displayed in Fig. 12.

From Table 2, it can be seen clearly that HCN, HNCO, and C_3H_3N are the major nitrogen-containing intermediates produced in both rich and lean pyrrole flames. Since pyrrole is a predominant nitrogenous component of coal and other low-rank fossil fuels, NO_x produced in the combustion of these fuels must be relative to the reactions of HCN, HNCO, and C_3H_3N. The formation pathways of these species are illustrated in Fig. 12. HCN is the main decomposition product of pyrrole through pyrrolyl and pyrrolenine. Miller et al. pointed out that HCN appears to be the major product when the fuel nitrogen is bound in an aromatic ring, which is in good agreement with our results as well. HNCO is produced from the direct oxidation of HCN and reactions of pyrrolyl/nonallylic cyanoradical (a-C_3H_4CN)/crotonitrile and O/OH. Compared with HCN and HNCO produced from several routes, 2-propenenitrile has a simple formation pathway, since it is produced mainly from crotonitrile, as presented in Fig. 12. In the following section, we will briefly discuss the consumption channels of these nitrogen-containing intermediates.

For HCN, thermal decomposition is unimportant in combustion because the C–H bond is very strong (about 520 kJ/mol) [42]. It can be consumed by acetylene and by OH and O radicals, as well as isomerization to produce HNC, corresponding to the reactions

$$C_2H_2 + HCN \leftrightarrow C_3H_3N, \quad (8)$$

$$OH + HCN \leftrightarrow HNCO + H, \quad (9a)$$

$$OH + HCN \leftrightarrow CN + H_2O, \quad (9b)$$

$$O + HCN \leftrightarrow NH + CO, \quad (10a)$$

$$O + HCN \leftrightarrow NCO + H, \quad (10b)$$

$$O + HCN \leftrightarrow CN + OH, \quad (10c)$$

$$HCN \leftrightarrow HNC, \quad (11a)$$

$$HNC + O \leftrightarrow HNCO \leftrightarrow NH + CO, \quad (11b)$$

$$HNC + OH \leftrightarrow HNCO + H, \quad (11c)$$

$$HNC + O_2 \leftrightarrow HNCO + O, \quad (11d)$$

$$HNC + O_2 \leftrightarrow NH + CO_2. \quad (11e)$$

It is realized that the mole fraction of HCN in the lean flame is lower than that in the rich flame, which results from the fact that it is easy for HCN to be consumed by oxygenous species in the lean flame. This is in accordance with previous study [47]. The isomerization barrier for HCN to HNC is about 200 kJ/mol. Lin et al. suggested that isomerization is an important reaction of HCN at high temperatures [67] and QRRK analysis indicated that the reaction occurs usually in

the low-pressure limit at temperatures above 1000 K and is important for HCN consumption in flame conditions [42]. Hence, HNC is concluded to be one of the major destruction products of HCN in the present work; and NH, CO, and NO are produced via HNCO, the dominant oxidation product of HNC.

According to the Gaussian-2 quantum chemical calculation, HNCO is the most stable among its isomeric structures [68]. HNCO is used as the active species in the "RAPRENO$_x$" NO$_x$ abatement process [39]. It is also predicted to be the major product of the reaction $CH_2 + NO$ [42]. HNCO participates in radical–molecule reactions and is mainly converted to NO, CO, and CO_2 through the reactions

$$HNCO + M \leftrightarrow NH + CO + M, \quad (12a)$$

$$HNCO + O \leftrightarrow HN(O)CO \leftrightarrow HNO + CO, \quad (12b)$$

$$HNCO + O \leftrightarrow HNC(O)O \leftrightarrow NH + CO_2, \quad (12c)$$

$$HNCO + OH \leftrightarrow NCO + H_2O \leftrightarrow NO, \quad (12d)$$

$$HNCO + H \leftrightarrow H_2 + NCO \leftrightarrow NO. \quad (12e)$$

The maximum mole fraction of HNCO in the lean flame is about three times that in the rich flame, which can increase the concentrations of NH, HNO, and CO_2 in the lean flame. NH and HNO could be the major precursors producing NO by the sequence shown in the reactions

$$NH + O_2 \leftrightarrow HNO + O, \quad (13a)$$

$$NH + O_2 \leftrightarrow NO + OH, \quad (13b)$$

$$HNO + OH \leftrightarrow NO + H_2O. \quad (14)$$

The nitric oxide formation from HNCO is responsible for the observation that the value of HNCO/NO near the burner surface is larger than unity, which is in agreement with the result of Miller and Bowman [46].

In the pyrrole flames, C_3H_3N can be consumed through the reactions with H/O/OH and the major products are HCN, HNCO, and C_2H_2:

$$H_2CCHCN + H \leftrightarrow HCCHCN + H_2, \quad (15a)$$

$$H_2CCHCN + H \leftrightarrow HCN + C_2H_3, \quad (15b)$$

$$H_2CCHCN + OH \leftrightarrow HCCHCN + H_2O, \quad (16a)$$

$$H_2CCHCN + OH \leftrightarrow HNCO + C_2H_3, \quad (16b)$$

$$H_2CCHCN + O \leftrightarrow HCCHCN + OH, \quad (17a)$$

$$H_2CCHCN + O \leftrightarrow HNCO + C_2H_2. \quad (17b)$$

The reactions (15b) and (16b) could be neglected in the pyrrole flame because C_2H_3 is not observed in this work. Moreover, HCCHCN may not exist in the flame since IE of HCCHCN (IE = 10.486 eV), calculated by the density functional B3LYP method using the 6-31G(d) basis set [65] in the present work, can hardly fit the onset on the PIE spectra of $m/e = 52$, which indicates that reactions (15a), (16a), and (17a) are not the main consumption pathways of C_3H_3N. Hence, reaction (17b) to produce HNCO and C_2H_2 is suggested as the most possible consumption pathway of C_3H_3N.

Besides HCN, HNCO, and C_3H_3N, other observed nitrogenous species such as CH_3N, CH_3NO, $C_2H_4N_2$, C_5H_7N, C_5H_9N, C_6H_5N, C_6H_9N, C_5H_5NO, $C_6H_{11}N$, C_5H_7NO, $C_6H_{13}N$, C_7H_5N, $C_6H_4N_2$, C_7H_7N, C_7H_9N, C_6H_7NO, $C_6H_{16}N_2$, and C_8H_7N have not been reported in previous pyrolysis/oxidation studies of pyrrole, even nitrogen-containing compounds. For most of these species, the formation and consumption pathways remains unclear. Their contribution to the formation of NO$_x$ and other pollutants in combustion of nitrogen-containing fuels requires confirmation from future modeling studies.

5. Conclusion

The experimental studies of low-pressure premixed pyrrole/O_2/Ar flames under lean ($\Phi = 0.55$) and rich ($\Phi = 1.84$) conditions have been performed with tunable synchrotron photoionization and molecular-beam mass spectrometry techniques. Isomers of intermediates in the two flames have been identified according to the measurements of photoionization efficiency spectra and photoionization mass spectra. The mole fraction profiles of major species and intermediates have been derived by scanning the burner position at selective photon energies near ionization thresholds. Flame temperature is measured by a Pt/Pt–13% Rh thermocouple. N_2, NO, and NO_2 are found to be the major nitrogenous products, while hydrogen cyanide, isocyanic acid, and 2-propenenitrile are the most abundant nitrogen-containing intermediates in pyrrole flames. Moreover, the reaction pathways in the pyrrole flames are briefly analyzed with a focus on the consumption of the major nitrogen-containing intermediates.

In comparison, a lot of intermediates such as 1,3-butadiyne, 1,3-butadiene, phenylnitrene, benzonitrile, 4-methylbenzyl radical, 2-vinylpyridine, indolizine, and *m*-tolunitrile exist only in the rich flame, while formamide, formic acid, isocyanoacetylene, isobutyl radical, 2-pentyn-4-one, 2,4-dimethyloxazole, cyclohexanamine, *N*-phenyl methanimine, and 6-methyl-2-pyridinol are observed only in the lean flame. Furthermore, concentrations of C_2H_2 and HCN in the rich flame are higher than in the lean flame, whereas HNCO is easily formed in the lean flame. The possible consumption reactions of HCN are acetylene-addition to the triple bond, hydrogen abstraction by OH, reaction with oxygen atom, and

isomerization to HNC. HNCO participates in radical addition and abstraction reactions and is mainly converted to NO, CO, and CO_2. And the main products from C_3H_3N are C_2H_2 and HNCO. The experimental results are useful for studying the conversion of volatile nitrogen compounds and understanding the formation mechanism of NO_x in flames of nitrogen-containing fuels.

Acknowledgments

The authors are grateful for funding support from the Chinese Academy of Sciences (CAS), the Natural Science Foundation of China under Grants 20473081 and 20533040, National Basic Research Program of China (973) under Grant 2007CB815204, the SRF for ROCS, and the SEM. The authors thank Dr. Bin Yang and Jing Wang for their helpful discussions.

References

[1] E.B. Higman, I. Schmeltz, W.S. Schlotzhauer, J. Agric. Food Chem. 18 (1970) 636–639.
[2] R.A. Jones, E.C. Taylor, A. Weissberger, Pyrroles: The Chemistry of Heterocyclic Compounds, Wiley, New York, 1990/1992.
[3] S. Wallace, K.D. Bartle, D.L. Perry, Fuel 68 (1989) 1450–1455.
[4] P.F. Nelson, A.N. Buckley, M.D. Kelly, Proc. Combust. Inst. 24 (1992) 1259–1267.
[5] L.R. Snyder, Anal. Chem. 41 (1969) 314–323.
[6] E. Ikeda, J.C. Mackie, J. Anal. Appl. Pyrol. 34 (1995) 47–63.
[7] M. Martoprawiro, G.B. Bacskay, J.C. Mackie, J. Phys. Chem. A 103 (1999) 3923–3934.
[8] M. Lumbreras, M.U. Alzueta, A. Millera, R. Bilbao, Combust. Sci. Technol. 172 (2001) 123–139.
[9] P.A. Mullen, M.K. Orloff, J. Chem. Phys. 51 (1969) 2276–2278.
[10] M. Bavia, F. Bertinelli, C. Taliani, C. Zauli, Mol. Phys. (1976) 479–489.
[11] A.J. van der Brom, M. Kapelios, T.N. Kitsopoulos, N.H. Nahler, B. Cronin, M.N.R. Ashfold, Phys. Chem. Chem. Phys. 7 (2005) 892–899.
[12] E.E. Rennie, C.A.F. Johnson, J.E. Parker, R. Ferguson, D.M.P. Holland, Chem. Phys. 250 (1999) 217–236.
[13] D.A. Blank, S.W. North, Y.T. Lee, Chem. Phys. 187 (1994) 35–47.
[14] J. Wei, A. Kuczmann, J. Riedel, F. Renth, F. Temps, Phys. Chem. Chem. Phys. 5 (2003) 315–320.
[15] B. Cronin, M.G.D. Nix, R.H. Qadiri, M.N.R. Ashfold, Phys. Chem. Chem. Phys. 6 (2004) 5031–5041.
[16] J. Wei, J. Riedel, A. Kuezmann, F. Renth, F. Temps, Faraday Discuss. 127 (2004) 267.
[17] A. Lifshitz, C. Tamburu, A. Suslensky, J. Phys. Chem. 93 (1989) 5802–5808.
[18] F. Dubnikova, A. Lifshitz, J. Phys. Chem. A 102 (1998) 10880–10888.
[19] J.C. Mackie, M.B. Colket, P.F. Nelson, M. Esler, Int. J. Chem. Kinet. 23 (1991) 733–760.
[20] T.A. Cool, K. Nakajima, T.A. Mostefaoui, F. Qi, A. McIlroy, P.R. Westmoreland, M.E. Law, L. Poisson, D.S. Peterka, M. Ahmed, J. Chem. Phys. 119 (2003) 8356–8365.
[21] T.A. Cool, A. McIlroy, F. Qi, P.R. Westmoreland, L. Poisson, D.S. Peterka, M. Ahmed, Rev. Sci. Instrum. 76 (2005) 094102.
[22] F. Qi, R. Yang, B. Yang, C.Q. Huang, L.X. Wei, J. Wang, L.S. Sheng, Y.W. Zhang, Rev. Sci. Instrum. 77 (2006) 084101.
[23] C.A. Taatjes, N. Hansen, A. McIlroy, J.A. Miller, J.P. Senosiain, S.J. Klippenstein, F. Qi, L.S. Sheng, Y.W. Zhang, T.A. Cool, J. Wang, P.R. Westmoreland, M.E. Law, T. Kasper, K. Kohse-Hoinghaus, Science 308 (2005) 1887–1889.
[24] C.Q. Huang, B. Yang, R. Yang, J. Wang, L.X. Wei, X.B. Shan, L.S. Sheng, Y.W. Zhang, F. Qi, Rev. Sci. Instrum. 76 (2005) 126108.
[25] C.Q. Huang, L.X. Wei, B. Yang, J. Wang, Y.Y. Li, L.S. Sheng, Y.W. Zhang, F. Qi, Energy Fuels 20 (2006) 1505–1513.
[26] B. Yang, C.Q. Huang, L.X. Wei, J. Wang, L.S. Sheng, Y.W. Zhang, F. Qi, W.X. Zheng, W.-K. Li, Chem. Phys. Lett. 423 (2006) 321–326.
[27] B. Yang, Y.Y. Li, L.X. Wei, C.Q. Huang, J. Wang, Z.Y. Tian, L.S. Sheng, Y.W. Zhang, F. Qi, Proc. Combust. Inst. 31 (2007) 555–563.
[28] B. Yang, P. Oßwald, Y.Y. Li, J. Wang, L.X. Wei, Z.Y. Tian, F. Qi, K. Kohse-Höinghaus, Combust. Flame 148 (2007) 198–209.
[29] M. Kamphus, N.N. Liu, B. Atakan, F. Qi, A. McIlroy, Proc. Combust. Inst. 29 (2002) 2627–2633.
[30] T.A. Cool, K. Nakajima, C.A. Taatjes, A. McIlroy, P.R. Westmoreland, M.E. Law, A. Morel, Proc. Combust. Inst. 30 (2005) 1681–1688.
[31] P.J. Linstrom, W.G. Mallard, NIST Standard Reference Database Number 69, 2003; http://webbook.nist.gov/chemistry.
[32] E. Ikeda, P. Nicholls, J.C. Mackie, Proc. Combust. Inst. 28 (2000) 1709–1716.
[33] J.A. Miller, M.D. Smooke, R.M. Green, R.J. Kee, Combust. Sci. Technol. 34 (1983) 149–176.
[34] C.P. Fenimore, G.W. Jones, J. Phys. Chem. 65 (1961) 298–303.
[35] J. Bian, J. Vandooren, P.J.V. Tiggelen, Proc. Combust. Inst. 21 (1986) 953–963.
[36] R.M. Green, J.A. Miller, J. Quant. Spectrosc. Radiat. Transfer 26 (1981) 313–327.
[37] R. Ancia, P.J.V. Tiggelen, J. Vandooren, Exp. Therm. Fluid Sci. 28 (2004) 715–722.
[38] A. Roger, A. Carlo, C. Maurizio, M. Anne, V. Yannick, B. Vincenzo, J. Am. Chem. Soc. 122 (2000) 324–330.
[39] R.A. Perry, D.L. Siebers, Nature 324 (1986) 657–658.
[40] J.D. Mertens, A.Y. Chang, R.K. Hanson, C.T. Bowman, Int. J. Chem. Kinet. 21 (1989) 1049–1067.
[41] C.H. Wu, H.T. Wang, M.C. Lin, R.A. Fifer, J. Phys. Chem. 94 (1990) 3344–3347.

[42] J.W.C. Gardiner, Gas-Phase Combustion Chemistry, Springer-Verlag, New York, 1999, pp. 197–285.
[43] E. Zervas, X.J. Montagne, Air Waste Manage. Assoc. 49 (1999) 1304–1314.
[44] C.P. Fenimore, Combust. Flame 26 (1976) 249–256.
[45] B.S. Haynes, Combust. Flame 28 (1977) 113–121.
[46] J.A. Miller, C.T. Bowman, Prog. Energy Combust. Sci. 15 (1989) 287–338.
[47] S. Koger, H. Bockhorn, Proc. Combust. Inst. 30 (2005) 1201–1209.
[48] J.A. Miller, C.F. Melius, Combust. Flame 91 (1992) 21–39.
[49] H. Che, H. Bi, R. Ding, D. Wang, L. Meng, S. Zheng, D. Wang, D.K.-W. Mok, F.-T. Chau, Chem. Phys. Lett. 382 (2003) 291–296.
[50] N.B. Feilchenfeld, W.H. Waddell, Chem. Phys. Lett. 98 (1983) 190–194.
[51] A.K. Schrock, G.B. Schuster, J. Am. Chem. Soc. 106 (1984) 5228–5234.
[52] M.S. Leyva, M.S. Platz, J.W.G. Persy, J. Am. Chem. Soc. 108 (1986) 3783–3790.
[53] D.A. Hrovat, E.E. Waali, W.T. Borden, J. Am. Chem. Soc. 114 (1992) 8698–8699.
[54] R.N. McDonald, S.J. Davidson, J. Am. Chem. Soc. 115 (1993) 10857–10862.
[55] W.L. Karney, W.T. Borden, J. Am. Chem. Soc. 119 (1997) 1378–1387.
[56] C.R. Kemnitz, W.L. Karney, W.T. Borden, J. Am. Chem. Soc. 120 (1998) 3499–3503.
[57] Z. Riedl, G. Hajós, W.J. Peláez, O.T. Gafarova, E.L. Moyano, G.I. Yranzo, Tetrahedron 29 (2003) 851–856.
[58] I.V. Tokmakov, G.S. Kim, V.V. Kislov, A.M. Mebel, M.C. Lin, J. Phys. Chem. A 109 (2005) 6114–6127.
[59] L. Zhai, X.F. Zhou, R.F. Liu, J. Phys. Chem. A 103 (1999) 3917–3922.
[60] G.B. Bacskay, M. Martoprawiro, J.C. Mackie, Chem. Phys. Lett. 300 (1999) 321–330.
[61] A.E. Axworthy, V.H. Dayan, G.B. Martin, Fuel 57 (1978) 29–35.
[62] O.S.L. Bruinsma, P.J.J. Tromp, H.J.J.d. Sauvage, J.A. Montijn, Fuel 67 (1988) 334–340.
[63] A. Doughty, J.C. Mackie, J. Phys. Chem. 96 (1992) 272–281.
[64] W.A. Rendall, M. Torres, E.M. Lown, O.P. Strausz, Rev. Chem. Intermediates 6 (1986) 335.
[65] Note: A B3LYP method with the 6-31G(d) basis set are used for structure optimization and energy calculations of pyrrolenine (C_4H_5N) and HCCHCN.
[66] C.Y. Oh, S.K. Shin, H.L. Kim, C.R. Park, J. Phys. Chem. A 107 (2003) 4333–4338.
[67] M.C. Lin, Y. He, C.F. Melius, Int. J. Chem. Kinet. 24 (1992) 1103–1107.
[68] W.A. Shapley, G.B. Bacskay, J. Phys. Chem. A 103 (1999) 6624–6631.